

Short range repulsive interatomic interactions in energetic processes in solids

J.M. Pruneda* and Emilio Artacho

Department of Earth Sciences, University of Cambridge Downing Street, Cambridge, CB2 3EQ, United Kingdom

(Dated: February 2, 2008)

The repulsive interaction between two atoms at short distances is studied in order to explore the range of validity of standard first-principles simulation techniques and improve the available short-range potentials for the description of energetic collision cascades in solids. Pseudopotentials represent the weakest approximation, given their lack of explicit Pauli repulsion in the core-core interactions. The energy (distance) scale realistically accessible is studied by comparison with all-electron reference calculations in some binary systems. Reference calculations are performed with no approximations related to either core (frozen core, augmentation spheres) or basis set. This is important since the validity of such approximations, even in all-electron calculations, rely on the small core perturbation usual in low-energy studies. The expected importance of semicore states is quantified. We propose a scheme for improving the electronic screening given by pseudopotentials for very short distances. The results of this study are applied to the assessment and improvement of existing repulsive empirical potentials.

PACS numbers: 71.15.-m, 71.15.Nc, 79.20.Ap, 61.80.-x, 34.20.Cf

I. INTRODUCTION

A high-energy ion (tens to hundreds of keV) propagating through the system can approach other atoms to very close distances, typically between 1 Å and 0.1 Å. The strong repulsive potential determines the scattering process. Ion implantation, laser ablation and displacement cascades produced by α -decay events in materials used for nuclear waste immobilization, are examples in which these energetic collisions play an important role. The energetic ion loses energy due to inelastic collisions with the electrons and other atoms in the material¹. The latter, called nuclear stopping, dominates for relatively low energies ($\lesssim 1$ keV/amu), while electronic stopping dominates for higher energies.

Nuclear stopping processes represent an enormous challenge because the kinetic energies involved allow for displacements of the atoms in large regions, and the energy dissipation takes place over long time scales (at least tens of picoseconds). Complicated structural configurations are obtained, with atoms breaking and making new bonds, and ionisation processes affecting the interactions between the particles. The complexity in physical and chemical interactions, the large sizes, and the long times involved in the problem demands high-efficiency first-principles calculations.

Many Density Functional Theory (DFT)² implementations used by the condensed matter community are based in the pseudopotential approximation, in which the core electrons are considered as frozen in their atomic configuration, and only the valence electrons are responsible of the chemical and physical properties of the solid, resulting in a substantial reduction of the degrees of freedom to be solved and hence in much faster calculations than the equivalent all-electron. For the very challenging problems in this area, it would be highly desirable to asses the usefulness and the range of validity of such approximation. It has to be remembered, however, that conventional

all-electron approaches are not much better suited for very short distances. If augmented plane waves (APW) are used to solve numerically the all-electron problem in the core region, problems arise when the augmentation spheres overlap. The need for an accurate basis set for the core electrons might prevent the use of available gaussian basis sets, normally devised for unperturbed core electrons.

Reference calculations are thus needed to test the accuracy of pseudopotential-based first principles calculations for describing electronic screening at short distances. Experimental uncertainties in the determination of the potentials are usually of the order of 10% or more. We have chosen to follow the approach of Nordlund *et. al.*³, and use as a reference calculations at the Hartree-Fock limit, where all these problems are eluded and the only remaining approximations are the absence of electronic correlation and of relativistic effects. In this work we have studied the relative importance of each of the effects that could be relevant to the problem, and assessed the validity of the pseudopotential approximation.

II. METHODOLOGY

For high energies the interatomic separation in a head-on collision can be small, making the binary collision (BC) an appropriate approximation. In this case, the complexities of the repulsive interaction between atoms can be modelled by a simple two-body interatomic potential for short distances. The interatomic potential $V(R)$ is defined as the difference between the total energy of the two atoms at a distance R , and the energy of the isolated atoms:

$$V(R) = E(R) - E(\infty) \quad (1)$$

We use two descriptions to characterize this potential: $\delta V(R)$, and the screening function $\Phi(R)$. The former is

defined as

$$\delta V(R) = V(R) - \frac{Z_1 Z_2 e^2}{R} \quad (2)$$

where Z_1 and Z_2 are the atomic numbers of the two atoms. This can be used to characterize the potentials at $r \rightarrow 0$. In the limit, we have the joint-atom solution, with just one atom with atomic number $Z_1 + Z_2$. Notice that $\delta V(0) = E^{atom}(Z_1 + Z_2) - E^{atom}(Z_1) - E^{atom}(Z_2)$, and we can use all-electron *atomic* calculations (without the problems related to basis commented before) to obtain information of this limit of the repulsive potential.

A different recasting of the interatomic potential that is also very useful⁴, is obtained if we consider the effect of screening due to the electronic cloud around the nuclei:

$$V(R) = \frac{Z_1 Z_2 e^2}{R} \Phi(R) \quad (3)$$

where $\Phi(R)$ is defined as the screening function. For very short distances, there is almost no screening of the internuclear repulsion because the probability of finding electrons in the interatomic region is very small, and $\Phi(0) \rightarrow 1$. For long distances the potential goes to zero faster than the Coulomb potential and $\Phi(\infty) \rightarrow 0$ (for neutral atoms). Some popular parametrizations of this potential⁵ are the ones due to Molière, Lenz-Jenson, Born-Mayer, and the one by Ziegler, Biersack and Littmark⁶ (ZBL). We will compare our results with the latter, that takes the form:

$$\Phi(R) = \sum_{i=1}^4 a_i e^{-b_i R} \quad (4)$$

where the numerical coefficients a_i and b_i are fitted to a variety of interatomic repulsive potentials for different pairs. This gives a relatively good agreement with experiment, specially for light elements. Nevertheless, the deviation with experimental ion scattering⁷ data can be as large as 20%.

The DFT energy $E(R)$ is obtained with the Siesta method⁸ using separable⁹ norm-conserving Troullier-Martins pseudopotentials¹⁰. The valence wave functions are expanded in pseudoatomic numerical orbitals including multiple- ζ and polarization function. Periodic boundary conditions require the definition of a supercell large enough for the interaction between replicas of the atoms to be sufficiently small ($L \sim 20\text{\AA}$). An uniform real-space grid defined by an equivalent plane-wave cutoff of 350 Ry was used for numerical integration.

In our simulations, scalar relativistic pseudopotentials are generated using different electronic configurations, including semicore states, partial core corrections, and different exchange-correlation functionals. The use of semicore shells, that is, core electrons considered as part of the valence, has the benefit of increasing the accuracy as compared to all-electron calculations, making the pseudopotential harder, and more demanding

computationally. In table I the different configurations used for core/valence electrons are shown. Partial core corrections¹¹ (PCC) account at least partially for non-linearity of the exchange-correlation functional due to the charge-density overlap between core and valence electrons. Notice that including scalar relativistic effects, as well as the correlation, represents, at least in some respects, an improvement to HF.

We compare the potentials obtained with Siesta with those obtained using the same numerical Hartree-Fock method as Nordlund *et. al.*³ and developed by Laaksonen *et. al.*¹². This HF approach, uses wave-functions of the general form:

$$\psi(\xi, \eta, \phi) = \frac{e^{im\phi}}{(2\pi)^{1/2}} u(\xi, \eta) \quad (5)$$

and the Hartree-Fock equations are reduced to partial differential equations for the function $u(\xi, \eta)$ in prolate spheroidal coordinates. The equations are then discretized using finite differences.

This numerical method is used as a reference in our electronic structure calculation. The effect of electronic correlation was shown not to be relevant, at least for the light element potential studied by Nordlund *et. al.*³. We confirm this result on other systems. We also checked that relativistic effects not included in the Hartree-Fock method, are important but not relevant for the purpose of this work. Thus, albeit the computational cost of HF restricts its application to relatively simple systems, it appears to be a good tool to gauge our approximation and test the accuracy achieved with other methods.

III. RESULTS

The pairs considered in this work were C-C, O-O, Si-Si, Ca-O, and Ca-Ca with both HF and DFT, and U-O with only DFT. The screening functions $\Phi(R)$ are shown in figures 1 and 2. Deviations from HF become relevant for distances $R \geq 0.7\text{\AA}$, when the attractive bonding interaction begins to be important. It is in this region of bonding character in the interatomic potential where the different descriptions of exchange and correlation give different results. It is, however, not important for this study. We used the Ceperley-Alder¹³ parametrization of exchange-correlation in the Local Density Approximation (LDA), and the Perdew, Burke and Ernzerhof¹⁴ scheme

TABLE I: Electronic configurations considered for the pseudopotential generation.

| | core | semicore | valence |
|----|---------------------------------------|---------------------------------|---|
| C | | 1s ² | 2s ² 2p ² |
| O | [He] | | 2s ² 2p ⁴ |
| Si | [He] 2s ² | 2p ⁶ | 3s ² 3p ² |
| Ca | [Ne] | 3s ² 3p ⁶ | 4s ² |
| U | [Xe]4f ¹⁴ 5d ¹⁰ | 6s ² 6p ⁶ | 7s ² 6d ¹ 5f ³ |

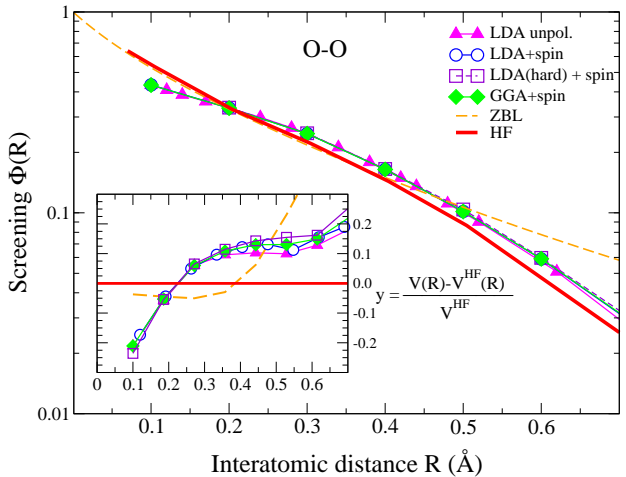


FIG. 1: (Color online) Screening function for O-O with different approximation for exchange-correlation (spin unpolarized LDA, spin polarized LDA and GGA, HF and ZBL). The reference configuration for the pseudopotential generation was $2s^22p^4$ with core radius $r_c = 0.61\text{\AA}$, except for the *hard* LDA, where $r_c = 0.53\text{\AA}$. The inset shows the ratio between the difference in computed potentials and the HF result.

for Gradient-corrected functional (GGA), both with and without spin polarization. We observed (Fig. 1) that any of these approximations for exchange and correlation gives essentially the same repulsive potential. The agreement with HF is good in general, even for short distances, showing that electronic correlation plays only a minor role in the repulsive potential. Note that ZBL gives a good description of the repulsive HF potential for light elements (C, O). For larger elements this agreement is not so good (see below).

A. Analysis of the different approximations

1. Effect of semicore states

In Fig. 2 we analyze the influence of semicore states in the screening. When the core electrons of one atom begin to overlap with the core electrons of the other atom, the Pauli repulsion between them is not properly taken into account in the pseudopotential approximation and consequently the result deviates from the Hartree-Fock description. The use of semicore states in the pseudopotential improves this, with part of the core included as valence. This can clearly be seen in the top Fig.2a, comparing the HF results with those obtained with pseudopotentials. In 2b, we observe the influence of these semicore states in the hardness/softness of the repulsive potential. The absence of semicore electrons in the valence, makes $V(R)$ softer. Fig.2c shows the deviation of the potential with respect to the HF value. Although this result was expected, it is important to quantify it with respect to

other effects, and to obtain an easy rule to assess the limit of validity of the pseudopotential approximation.

When the interatomic distance is comparable to bonding distances ($R \sim 1\text{\AA}$), the valence electrons are spread around the atoms and in the bonding region, screening the Coulomb interaction between the nuclei. As the distance between the nuclei is reduced, the repulsive electronic interactions (Coulomb and Pauli) in the bonding region increase, and the electrons are more unlikely to be in the confined area between the nuclei. This is shown in Fig. 3, where the valence charge distribution around the atoms is displaced from the interatomic center, to the surrounding area as the distance decreases. In a simulation within the pseudopotential approximation, the valence electrons have a smaller participation in the nuclear screening, but the core electrons are assumed to be fixed in their initial configuration, and thus, their contribution to the screening is roughly the same. For this reason $\Phi(R)$ is always smaller than the expected screening function with an *all electron* approach.

Core electrons deep in the inner shells (see Fig.2d), are more strongly bonded to the nuclei and their participation in the collision would only be relevant for very high collision energies when the interatomic distance becomes really small. For that energy scale, the electronic stopping power is more important than the nuclear stopping power. Hence, an accurate description of the repulsive potential for shorter (higher) distances (energies), is beyond the scope of this study.

Only the outer core-shell electrons are included in the semicore. How localized these electrons are can be roughly estimated using the spread of the corresponding atomic Kohn-Sham orbitals in a DFT all-electron calculation. In table II we show for each atomic shell, the radii r_{90} and r_{99} , in which 90% or 99% of the atomic wavefunction's norm is localized. Two shells corresponding to different atoms will likely interact, if the interatomic distance is smaller than sum of the radii at which the charge is more localized. According to this, and considering r_{90} as a reference, in a Si-Si collision, we can say that 2s electrons will interact with 2s or 2p valence electrons in the other atom for distances $R \lesssim 0.95\text{\AA}$, which is an appreciable distance (see arrows in Fig.2a). So, if we want to have a good description of the collision for shorter ranges, we would need to include 2s electrons into the semicore. With that, we would ensure a reasonable description of the interactions up to distances of the order of 0.2\AA , when the 1s electrons start to play a role. This would explain why the pseudopotential without any semicore state gives such a soft repulsive potential.

The same argument may be used for 1s electrons in a C-C collision for distances smaller than 0.4\AA , and for the 2s-2p electrons in a Ca-Ca collision below $\sim 0.6\text{\AA}$. In the Ca-Ca case, both the 3s and 3p shells have to be included in the semicore for reasonable screening down to $2r_{90}$, in accordance to the model. In Si-Si, however, the 2p electrons seem to be enough, and the 2s apparently do not affect the screening for distances smaller than $\sim 1\text{\AA}$.

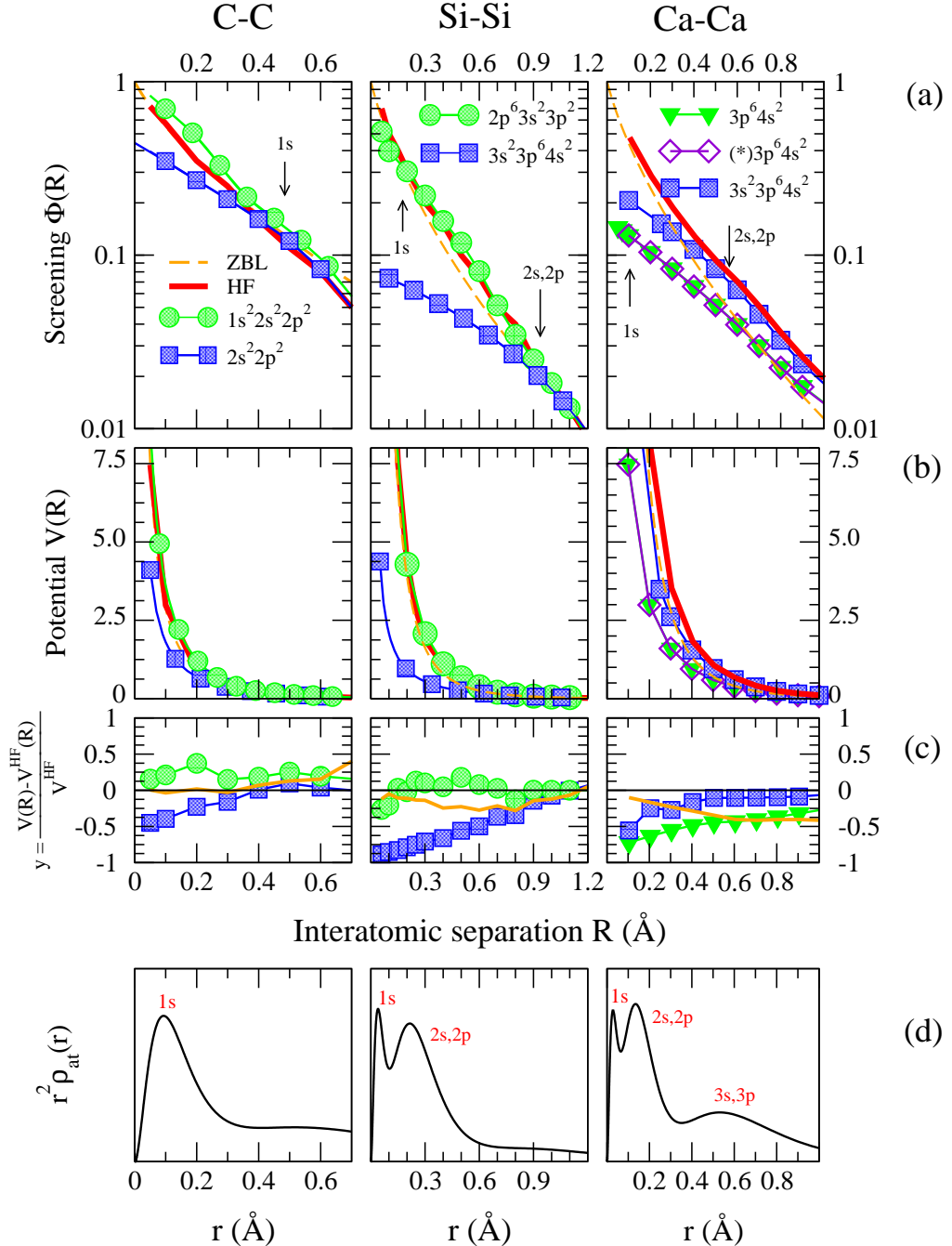


FIG. 2: (Color online). (a) Screening function for C-C, Si-Si and Ca-Ca, with different electronic configurations for the pseudopotential. (b) Interatomic repulsive potential $V(R)$ in keV. (c) Deviation of the potential with respect to the HF limit. (d) Charge distribution, $r^2 \rho(r)$, showing the core electronic shells. $(*)3p^64s^2$ differs from $3p^64s^2$ just in the number of ζ 's used to describe the 3p orbitals (double- ζ , and single- ζ respectively). The small arrows in (a) show the distance at which electronic clouds from the core start to overlap with each other ($R=2r_{90}$, see table II).

2. Effect of the core radius

In the pseudopotential approximation, it is assumed that the core electrons of different atoms do not overlap.

For the interatomic distances of interest in this work, this is not the case. Although the core radii of the pseudopotentials (r_c) play an important role in the description of ground state properties of real materials, the effects for

TABLE II: Radii (in Å) containing 90% or 99% of the total charge for each atomic orbital for C, O, Si and Ca. Core electron eigenenergies (ϵ in eV) are also shown as computed with an all-electron atomic DFT, as well as experimental values for the corresponding binding energies¹⁵.

| C | | | | O | | | | Si | | | | Ca | | | | | | | |
|-------|----------|----------|------------|-------|-------|----------|----------|------------|-------|-------|----------|----------|------------|-------|----------|----------|------------|-------|-------|
| shell | r_{90} | r_{99} | ϵ | E_B | shell | r_{90} | r_{99} | ϵ | E_B | shell | r_{90} | r_{99} | ϵ | shell | r_{90} | r_{99} | ϵ | E_B | |
| 1s | 0.26 | 0.42 | -273 | -284 | 1s | 0.19 | 0.31 | -514 | -543 | 1s | 0.11 | 0.17 | -1774 | -1839 | 1s | 0.07 | 0.12 | -3929 | -4038 |
| 2s | 1.34 | 2.06 | -14 | | 2s | 0.98 | 1.51 | -24 | -41 | 2s | 0.47 | 0.70 | -160 | -149 | 2s | 0.30 | 0.44 | -412 | -438 |
| 2p | 1.64 | 2.71 | -5 | | 2p | 1.17 | 1.96 | -9 | | 2p | 0.48 | 0.77 | -117 | -100 | 2p | 0.29 | 0.44 | -326 | -349 |
| | | | | | | | | | | 3s | 1.55 | 2.17 | -28 | | 3s | 0.92 | 1.32 | -47 | -44 |
| | | | | | | | | | | 3p | 1.04 | 1.55 | -28 | | 3p | | | | -25 |

the repulsive potential at short distances is not as dramatic. Changes of up to 40% in r_c give differences in the repulsive potentials smaller than 2% when the interatomic distance is smaller than $2r_c$, whereas differences can be as large as 20% when the distance is close to $2r_c$.

3. Effect of charge state, correlation, and relativistic corrections

The charge state of the shooting ion can play an important role in the description of the electronic energy loss for intermediate energies. For the short range interatomic repulsion, however, these effects are not so relevant: since electrons move out of the internuclear region for short interatomic distances (Fig. 3), there will be no important effect on the repulsive potential if the ionization involved not too deep electrons.

Correlation and relativistic corrections are known to be relevant for very short distances or very heavy nuclei. In the pseudopotential method, scalar relativistic corrections are included, but not in the HF approach

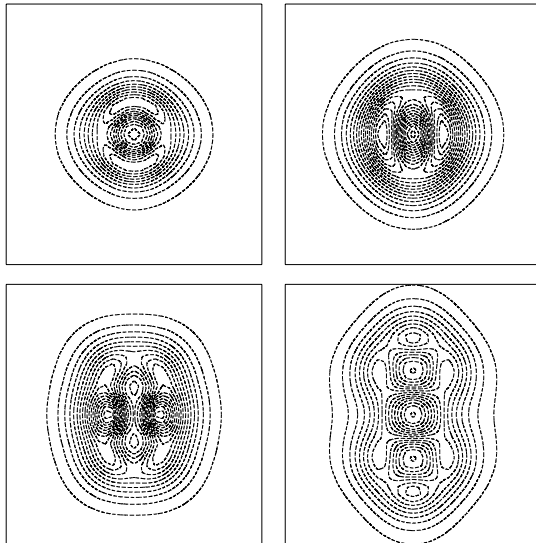


FIG. 3: Contour plot for the charge distribution at different interatomic distances for the Ca-Ca pair (0.1, 0.3, 0.5 and 1 Å, going from left to right and up to down).

that we use as a reference. With an all-electron DFT-based *atomic* calculation which includes relativistic effects (scalar and spin-orbit), we use $\delta V(0)$ to estimate an upper limit of the relativistic corrections. As an example a limit of ~ 1.3 keV is obtained in a Ca-Ca collision. Although this is a considerable correction, the energy scales we are interested in (see Fig. 4), are of the order of tens of keV. Furthermore, the relativistic effects

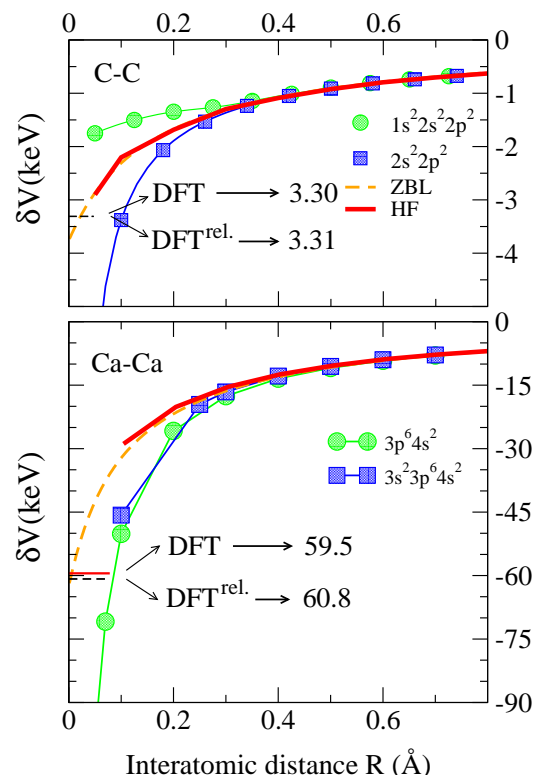


FIG. 4: (Color online) Non-coulombic interaction, $\delta V(R)$, for C-C (top) and Ca-Ca (bottom), and comparison with relativistic effects. The solid ticks at ~ 3.3 keV (for C-C) and ~ 60 keV (Ca-Ca) represent the atomic energy of Mg and Zr (atomic numbers twice as big as C and Ca) with an *all-electron* atomic DFT. The dashed tickmark represents the atomic energy with relativistic corrections (for C if falls over the solid lines in the energy scale used).

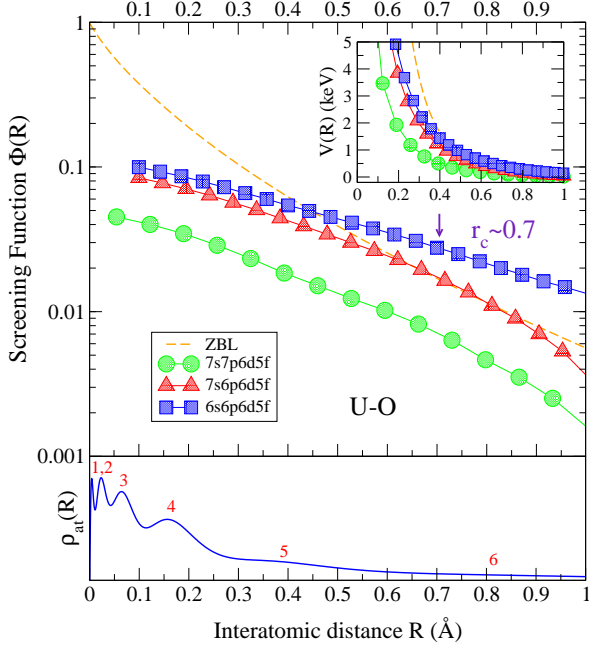


FIG. 5: (Color online) Screening function, $\Phi(R)$, and repulsive interatomic potential, $V(R)$ in the inset, for the U-O pair. The arrow shows the radius at which the $n=5$ shell of U overlaps with the $n=1$ shell of O. Bottom figure represents the electronic charge distribution for U, as computed with an atomic all electron DFT method.

are expected to be smaller for distances $\gtrsim 0.4\text{\AA}$. The difference between DFT and HF (both relativistic or both non-relativistic) is of the order of ~ 5 eV and gives an idea of the magnitude of correlation effects. It is evident from the figure that the approximations involved in the pseudopotential approach are much more relevant than correlation or relativistic effects.

B. Practical realization: Heavy ions

We can now try to obtain some qualitative information about the interatomic potential for heavy ions. The use of pseudopotentials for equilibrium (low energy) situations of lanthanide and actinide compounds has been shown to be accurate^{16,17} when the effects coming from overlap between core and valence are properly treated (either with the inclusion of semicore states, or with partial core correction), even if only scalar relativistic corrections are considered. Relativistic spin-orbit terms can also be important in these elements, and the results obtained within this method should be taken with caution.

We have computed the uranium-oxygen interatomic potential $V(R)$ with different pseudopotentials, and compared it to ZBL (see Fig. 5). The electronic configuration is shown in table I, and the localization radii r_{90} and r_{99} , in table III. Using the same arguments as be-

fore, we could expect that using a semicore with 6s and 6p electrons in the valence, the U-O interatomic potential obtained would be appropriate up to distances of the order of 0.7\AA . Note that the ZBL potential would give a lower screening than expected (at least for distances larger than 0.7\AA), giving a harder description of the binary collision.

C. Correction of the screening function

A systematic feature of the pseudopotential calculations is that in the limit of small distances, the screening functions obtained do not approach unity. This is due to the frozen core approximation and the fact that the inner shells of the electronic cloud are not contributing to the screening. We propose a method improve Φ by adding a continuous function that gives the proper limit ($\Phi(0) \rightarrow 1$) for values below the radius r_0 at which the core states begin to overlap. By inspection of figures 2 and 5 we could use the simplest function $\Phi(R) = e^{\alpha R^2 + \beta R}$, with parameters α and β fixed by the conditions over $\Phi(r_0)$ and $\frac{d\Phi}{dR}(r_0)$, giving continuity of the screening and its derivative (and thus, the interatomic force) at r_0 . Notice that the matching radii would depend on the particular configuration used for the generation of the pseudopotential. We propose to use the sums of the r_{90} for the relevant core states of both atoms considered: $r_0 = r_{90}^{atom1} + r_{90}^{atom2}$. In figure 6 we compare the previous screening functions with the ones corrected with this scheme. This will allow realistic molecular dynamic simulations with pseudopotentials, even if the atoms get extremely close in a high energy collision. Numerical fits of these potentials have already been used to do semiempirical simulations of collision cascades for studies of radiation damage in CaTiO_3 ¹⁸.

IV. CONCLUSIONS

The validity of the pseudopotential approximation has been checked at close distances as found in high energetic collisions in materials. We have compared the interatomic repulsive potential computed with an all-electron Hartree-Fock method, with that obtained with pseudopotentials. In this HF reference method, no approximation is assumed with respect to the core shells, or the basis used to represent the electronic states. The validity of the HF approximation itself has been assessed in order to use it as a reference for the pseudopotentials. The effect of different approaches to treat the electronic correlation was previously shown³ not to give substantial differences in the screening function, a result confirmed in this study. The relativistic corrections, though important, can be considered small for the energy scales of interest in this work.

It has been shown that as the nuclear distance decreases, the electrons are expelled from the internuclear

region to the surrounding area, and the screening is completely dominated by the deeper electrons, bound at short length scales. If the core is frozen at length scales longer or comparable to the internuclear distance, the screening is larger than expected and the pseudopotential description fails. We have shown this effect to be the most important one in the problem, actually the only one of relevance at the energy scales involved.

We have quantified to what extent the use of deeper electrons as part of the valence configuration is essential to describe the repulsive potential for relatively short internuclear distances. The localization of the core electrons, r_{90} , has been found as the most appropriate criterion used to decide which states have to be included for a particular range of collision energies. The pseudopotential description would then be valid until the more external core shells not included in the calculation

start to overlap. Finally, we have proposed a scheme to correct the screening given in the pseudopotential approximation, that recovers the right trend for very short distances, and improves the use of pseudopotentials for the description of energetic collisions with first principles simulations.

V. ACKNOWLEDGMENTS

This work was supported by British Nuclear Fuels (BNFL) and NERC. We would like to thank M. Dove, K. Trachenko for helpful discussions and sharing their experience with MD methods in radiation damage simulations.

* Corresponding Author: mpru02@esc.cam.ac.uk

¹ N. Bohr, Philos. Mag. **25**, 10 (1913).

² P. Hohenberg and W. Kohn, Phys. Rev. **136**, B864 (1964); W. Kohn and L. J. Sham, Phys. Rev. **140**, A1133 (1965).

³ K. Nordlund, N. Runeberg, and D. Sundholm, Nucl. Instr. and Meth. B **132**, 45 (1997).

⁴ R. Smith, M. Jakas, D. Ashworth, B. Oven, M. Bowyer, I. Chakarov, and R. Webb, *Atomic and ion collisions in solids and at surfaces. Theory, simulation and applications* (Cambridge University Press, 1997).

⁵ I. M. Torrens, *Interatomic Potentials* (Academic Press, New York, 1972).

⁶ J. F. Ziegler, J. P. Biersack, and U. Littmark, *The Stopping and Range of Ions in Solids* (Pergamon Press, New York, 1985).

⁷ G. H. Lane, and E. Everhart, Phys. Rev. **120**, 2064 (1960).

⁸ P. Ordejón, E. Artacho, and J. M. Soler, Phys. Rev. B **53**, 10441 (1996); J. M. Soler, E. Artacho, J. D. Gale, A. García, J. Junquera, P. Ordejón and D. Sánchez-Portal, J. Phys.: Condens. Matter **14**, 2745 (2002).

⁹ L. Kleinman and D.M. Bylander, Phys. Rev. Lett. **48**, 1425 (1982).

¹⁰ N. Troullier and J. L. Martins, Phys. Rev. B **43**, 1993 (1991).

¹¹ S. G. Louie, S. Froyen, and M. L. Cohen, Phys. Rev. B **26**, 1738 (1982).

¹² J. Kobus, L. Laaksonen, D. Sundholm, Comp. Phys. Commun. **98**, 346 (1996).

¹³ D. M. Ceperley and B. J. Alder, Phys. Rev. Lett. **45**, 566 (1980).

¹⁴ J. P. Perdew, K. Burke, M. Ernzerhof, Phys. Rev. Lett. **77**, 3865 (1996).

¹⁵ <http://www.webelements.com/> by M. Winter, and references therein.

¹⁶ C. J. Pickard, B. Winkler, R. K. Chen, M. C. Payne, M. H. Lee, J. S. Lin, J. A. White, V. Milman, D. Vanderbilt, Phys. Rev. Lett. **85**, 5122 (2000).

¹⁷ J. A. Alford, M. Y. Chou, E. K. Chang, and S. G. Louie, Phys. Rev. B **67**, 125110 (2003).

¹⁸ K. Trachenko, M. Pruneda, E. Artacho and M. T. Dove, submitted to Phys. Rev. B.

TABLE III: Estimated radii (\AA) for the localization of electronic orbitals in U, eigenenergies (eV) as obtained in an atomic DFT calculation, and electron binding energies (eV)¹⁵.

| shell | r_{90} | r_{99} | ϵ | E_B | shell | r_{90} | r_{99} | ϵ | E_B | shell | r_{90} | r_{99} | ϵ | E_B | shell | r_{90} | r_{99} | ϵ | E_B |
|-------------------|----------|----------|------------|---------|-------------------|----------|----------|------------|-------|-------------------|----------|----------|------------|-------|-------------------|----------|----------|------------|-------|
| 1s | 0.01 | 0.02 | -114939 | -115606 | 3p _{3/2} | 0.12 | 0.17 | -4222 | -4303 | 4d _{3/2} | 0.28 | 0.38 | -762 | -778 | 5p _{3/2} | 0.59 | 0.79 | -205 | -192 |
| 2s | 0.05 | 0.07 | -21496 | -21757 | 3d _{3/2} | 0.11 | 0.16 | -3674 | -3728 | 4d _{5/2} | 0.28 | 0.39 | -720 | -736 | 5d _{3/2} | 0.67 | 0.93 | -116 | -103 |
| 2p _{1/2} | 0.04 | 0.06 | -20731 | -20948 | 3d _{5/2} | 0.11 | 0.16 | -3496 | -3552 | 4f _{5/2} | 0.29 | 0.42 | -391 | -388 | 5d _{5/2} | 0.69 | 0.97 | -108 | -94 |
| 2p _{3/2} | 0.05 | 0.07 | -16961 | -17166 | 4s | 0.24 | 0.33 | -1395 | -1439 | 4f _{7/2} | 0.29 | 0.43 | -380 | -377 | 6s | 1.11 | 1.51 | -60 | -44 |
| 3s | 0.11 | 0.15 | -5440 | -5548 | 4p _{1/2} | 0.24 | 0.33 | -1238 | -1271 | 5s | 0.50 | 0.67 | -320 | -321 | 6p _{1/2} | 1.26 | 1.74 | -43 | -27 |
| 3p _{1/2} | 0.11 | 0.15 | -5092 | -5182 | 4p _{3/2} | 0.27 | 0.37 | -1011 | -1043 | 5p _{1/2} | 0.52 | 0.71 | -259 | -257 | 6p _{3/2} | 1.42 | 1.99 | -34 | |

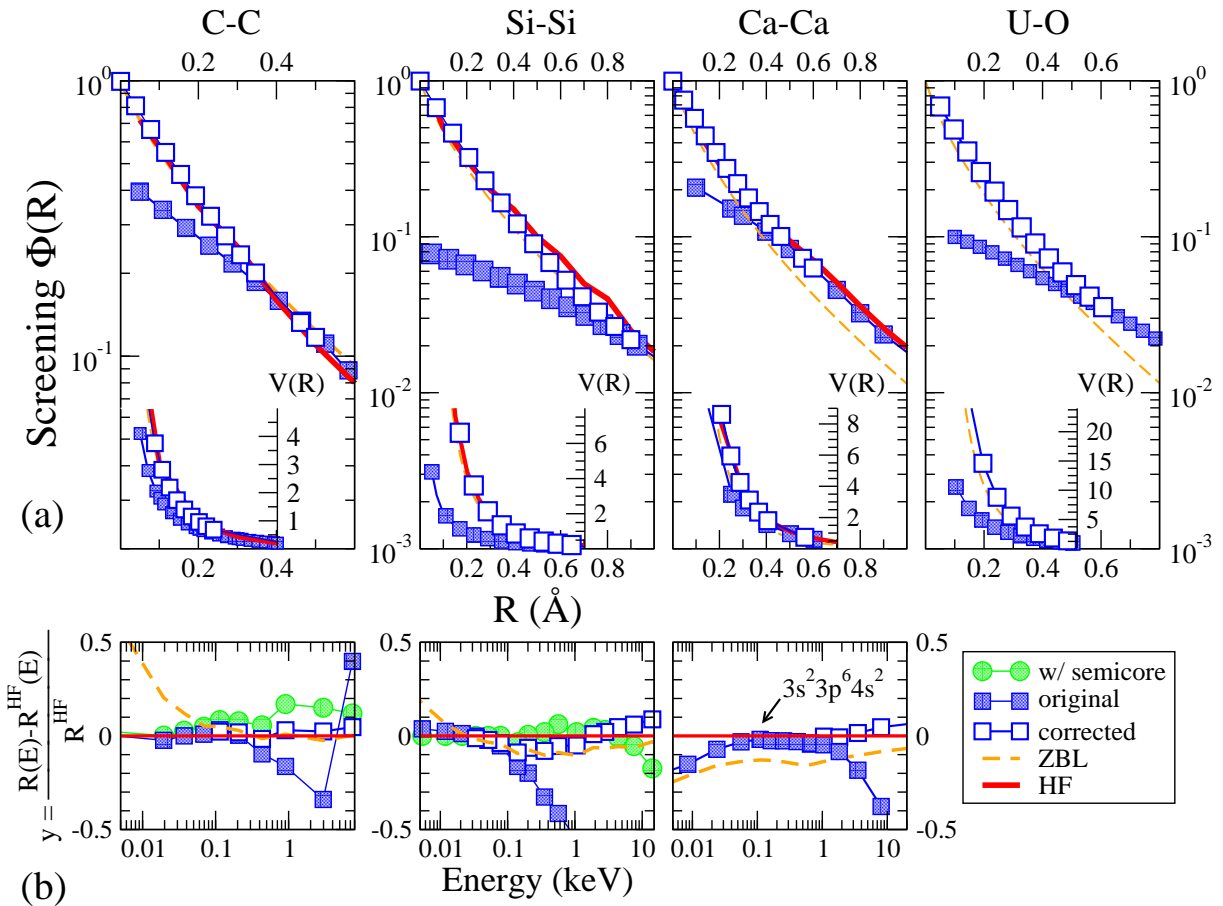


FIG. 6: (Color online). (a) Interatomic screening function for different pairs with the correction scheme proposed as compared with previous results. (b) Relative deviation with respect to HF in the internuclear distance corresponding to each energy. We compare the results obtained for: (1) the pseudopotentials without semicore (original); (2) with the correction proposed in this work (open square symbols); (3) the pseudopotential with semicore states; and (4) the ZBL parametrization. Note that considerable deviations in (1) appear for energies of hundreds of eV, and this is considerably improved with (2). ZBL gives good description of the high energy regime, but fails for energies smaller than ~ 0.1 keV.